Experimental Analysis of Engine Characteristics of Spark Ignition Engine Fuelled By Low Cetane Fuel

R. Narayanamoorthy[1], S. Sivaprakasam[2], P. Sivaraj[3]

[1]*Research Scholar & Assistant Professor, Department of Mechanical Engineering, Faculty of Engineering and Technology, Annamalai University, Tamilnadu – 608002, India*

[2]*Professor, Department of Mechanical Engineering, Faculty of Engineering and Technology, Annamalai University, Tamilnadu – 608002, India*

[3]*Associate Professor, Department of Manufacturingl Engineering, Faculty of Engineering and Technology, Annamalai University, Tamilnadu – 608002, India*

[1]rnm.lme@gmail.com, [2]rgssiva2002@gmail.com, [3]cemajorsiva@gmail.com

Abstract - *To reduce the dependency on fossil fuel-derived petroleum energy sources, the vegetable oil obtained from plant-based products can be regarded as potential alternate bioenergy sources. In this work, the bio-oil with low viscosity and low cetane number is tried as an alternative to gasoline fuel to study their effect on a spark-ignition engine's performance, emission, and combustion characteristics. The camphor oil (CMO) extracted from the woods of the camphor tree is used as a partial substitute to gasoline by blending it with gasoline in the ratio proportions of 10:90, 20:80, 30:70, and 40:60 by volume. Initially, the fuel properties are measured for camphor oil, and a blend stability test is performed on camphor test blends to study their suitability as a fuel. Then the experimental study is performed with camphor oil blends to analyze their effect on the engine characteristics. The results show that the 10% camphor oil blend's performance is comparable to that of gasoline. The BTE of CMO10 is 26.54% at full load, which is lesser than gasoline, whose BTE is 26.82%. For the same load, the NOx emission of CMO10 decreased by about 3% whereas CO and HC emission slightly increased by about 1.2% and 2% compared to that of neat gasoline. The experimental analysis found that camphor oil can be used up to 10% as a blend with gasoline fuel. Even though the performance of CMO10 is very slightly lesser than gasoline, it can be used with slight engine modifications to give gasoline-like efficiency.*

Keywords: *Alternate Fuel, Blend, Brake thermal efficiency, Camphor oil, Gasoline*

I. INTRODUCTION

In the road transportation sector, Gasoline and Diesel engines are the most commonly used prime movers globally. For the past 2 decades, when it comes to a light-duty passenger vehicle, the market of diesel engine cars have been significantly higher when compared to gasoline engine cars because of better fuel efficiency, lower maintenance cost, and lesser fuel price [1,2]. Especially in a country like India, where half of the country's population belongs to the economic class, most people prefer to buy diesel engine cars. Currently, the trend has been reversed after the implementation of BS-VI emission norms in April 2020 [3]. The NOx and Soot emission are major concerns with diesel engines, which negatively impact the environment, causing various health effects [4,5].

To meet the stricter BS-VI norms, Diesel engines need either engine up-gradation or after treatment methods. Since the technological up-gradation in the engine side to curb the emission is almost got saturated, the automobile manufacturers and researchers turn towards developing newer and optimization of existing after treatment technologies [6]. These after-treatment techniques add up a significant amount to diesel cars' overall cost and make their cost higher than gasoline cars [7]. Simultaneously, modern-day gasoline engines with a 3-way catalytic converter are very effective in meeting the BS-VI emission standards. Also, the price gap between gasoline and diesel fuel is reduced drastically [8]. These factors drive the people towards buying gasoline cars in the coming years. In this trend, gasoline usage and demand can rise steeply in the coming days [9].

On the other hand, the greenhouse gas (CO_2) emission from automobiles also possess a major threat to the environment by causing global warming and climatic changes [10,11]. The oil extracted from plant/crop-based biomass or various parts of a tree can be regarded as renewable and sustainable alternative fuels to reduce fossil fuel-based petroleum products' dependency. The plant's natural ability to absorb the CO_2 gas makes them a CO_2 sink [12]. Generally, fuels with high octane numbers are selected as an alternative to gasoline fuel to overcome the knocking tendency and improve thermal efficiency [13]. Alternate fuels such as lower order alcohols, LPG, and others are already experimentally proven as gasoline substitutes [14,15]. The researchers are currently trying to use bio-oils

with low viscosity cum low cetane (LVLC) number fuel property as a gasoline substitute in a spark-ignition engine. These special bio-oils can be used directly as fuel without converting raw oil into methyl esters [16]. This includes pine oil, the oil obtained from peels such as orange peel oil and lemon peel oil. Babu et al. experimental results proved that blending pine oil with gasoline up to 20% by volume improved the engine performance without any knocking tendency [17]. Terpineol, extracted from pine tree resin, has shown a higher octane rating than conventional gasoline. The terpineol 30% blend displayed increased combustion peak pressure when compared to gasoline [18]. Biswal et al. [19] and Velavan et al. [20] experimental studies of PFI engine powered by lemon peel oil (LPO) blends have found that the LPO blends improved the combustion characteristics, increased the engine BTE slightly, and reduced the HC, CO emissions when compared to sole gasoline.

From the literature survey, it is observed that no work has been reported on camphor oil as a partial substitute for gasoline fuel. Therefore, in this work, the camphor oil, obtained from the wood of the Cinnamomum camphora tree, which belongs to LVLC, has been tried as a partial substitute to gasoline fuel to find out its effects on the engine characteristics of MPFI system installed spark-ignition engine. The CMO was blended to sole gasoline in various proportions. Their impact on the combustion peak pressure, brake thermal efficiency, and harmful emission constituent present in the exhaust gases at various engine load conditions such as 1.6, 3.2, 4.8, 6.4, and 8 kW were studied.

II. FUEL PREPARATION AND PROPERTIES

The camphor oil is extracted from the camphor tree woods/leaves through the steam distillation process. When China, Taiwan, southern parts of Japan, Korea, and Vietnam [21]. In India, It is distributed in the windward evergreen forests of Agasthyamalai phytogeographical region, Kerala. It has been classified into four grades [16] by the fractional distillation process. Among the four, white camphor oil is taken for the study. But in this work, CMO extracted from camphor tree leaves was bought commercially from India's local market.

Table 1a. Fuel properties of gasoline and CMO measured as per ASTM Standards

Properties	Gasoline [22]	Camphor Oil [21]
Molecular Formula	C_2-C_{14}	$C_{10}H_{16}O$
Heating value (MJ/kg)	46.9	42.4
Octane number	90	-
Cetane number	-	5
Autoignition temperature (°C)	420	466
Enthalpy of vaporization (kJ/kg)	223	358
Boiling point (°C)	25-215	204
Density @ 20°C (kg/m³)	744.6	894.2
Oxygen Content (%)	0	10.5
Flash point (°C)	-38	46
Viscosity (mm²/s)	1.04	1.97

Table 1b. Fuel properties of CMO blends

Properties	CMO10	CMO20	CMO30	CMO40
Heating value (MJ/kg)	46.41	46.22	46.20	45.82
Density @ 20°C (kg/m³)	0.7431	0.7483	0.7526	0.7622
Flashpoint (°C)	-24	-22	-21	-21
Viscosity (mm²/s)	1.36	1.39	1.40	1.42

Initially, a Miscibility and phase separation test was conducted for camphor oil (CMO). A 100 ml of CMO was taken and mixed well with 500 ml of sole gasoline and kept at room temperature for 14 days. It was observed that CMO had shown good miscible nature with gasoline, and also no phase separation was observed during that period. The various fuel properties were measured according to ASTM standards for gasoline and CMO blends and given in table 1.

From the fuel properties of CMO oil, it is observed that its calorific value is approx. 84% of sole gasoline, which is very higher than ethanol. The enthalpy of vaporization of CMO oil is comparable to gasoline, so cold starting ability will not be affected as in ethanol. The higher auto-ignition temperature of CMO compared to gasoline helps to overcome the engine knocking. Even though the viscosity of CMO is higher than gasoline, the viscosity of CMO blends is still under the gasoline engine standards. The fuel flow and spray pattern will be affected slightly due to the high viscosity and density nature of CMO oil. Higher boiling and flash point of CMO adversely affects the evaporation process compared to gasoline. Further, the presence of an oxygen atom in the CMO molecular structure reduces CO and HC emissions. The details about the test blend preparations and their designations were given in table 2.

Table 2. Test Fuel Designations

Composition (Blends made based on volume proportions)	Designation
100% gasoline	Gasoline
90% gasoline + 10% CMO	CMO10
80% gasoline + 20% CMO	CMO20
70% gasoline + 30% CMO	CMO30

III. GC_MS STUDY OF CAMPHOR OIL

The GC_MS study of camphor oil was performed to find out the constituents present in it, and it is shown in figure 1. The intensity vs. retention time graphs helps to identify the various constituents present in the camphor oil. The key compounds present in the camphor oil are identified and listed in table 3 by matching their corresponding retention time with the compounds present in the mass spectral library. The results showed the strong presence of aliphatic and aromatic hydrocarbons in the camphor, making it possible to replace the fossil fuel-based fuels partially. ll paragraphs must be indented. All paragraphs must be justified, i.e., both left-justified and right-justified.
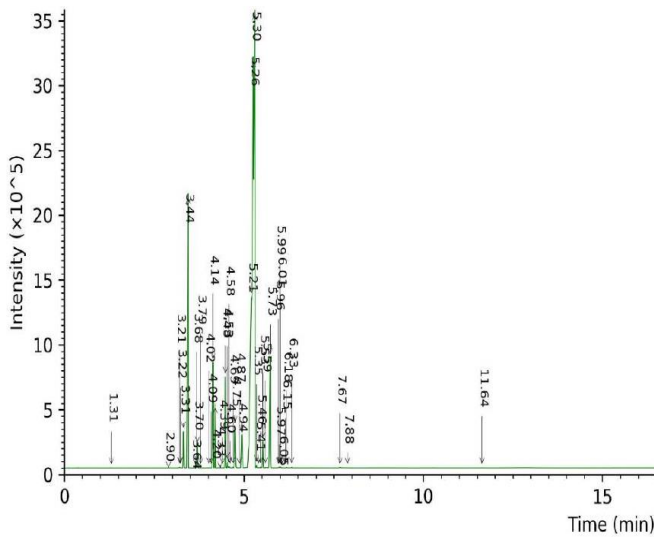

Fig. 1 Camphor oil GC_MS study

Table 3. Key Components present in the Camphor oil

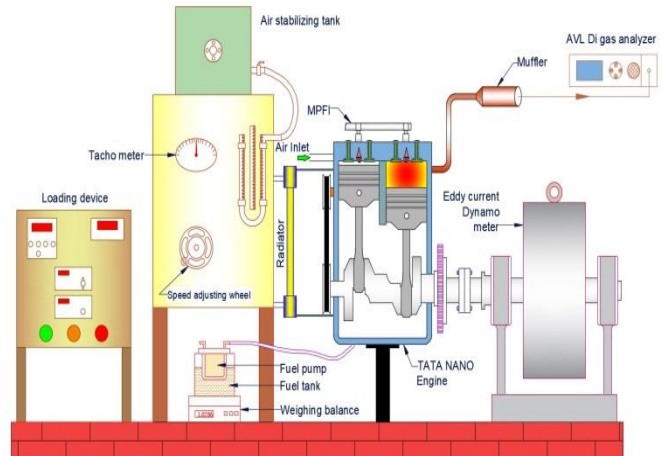| Key constituents in Camphor oil	Retention time (min)	%
Limonene	5.26	26.9
1,8-Cineole	5.30	25.4
p-Cymene	5.21	15.5
α-Pinene	3.44	12.3
γ-Terpinene	5.73	4.3
Sabinene	4.14	3.8
Myrcene	4.48	3.2
β-Pinene	4.20	2.0
α-Terpinene	4.94	1.6
α-Phellandrene	4.75	1.4
α-Thujene	3.31	1.2

IV. EXPERIMENTAL SETUP

Fig. 2 Research Engine Setup

The engine characteristic study was performed on a four-stroke, two-cylinder, water-cooled, spark-ignition engine having an MPFI system. The fuel was injected at an injection pressure of 5 bar. The engine specifications are given in table 3. The load on the engine was varied by eddy current dynamometer. The dynamometer was cooled by supplying water continuously at a constant rate. The engine speed was maintained constant at 2500 rpm by adjusting the throttle manually at the load conditions taken for the study. An electronic weighing machine was used to measure the amount of fuel consumed at each load condition. AVL measured the constituents such as HC, CO, NO in the exhaust gases make di-gas analyzer. The spark timing was set at a crank angle that corresponds to MBT. The time taken for the fuel consumption was noted with the help of a stopwatch. The in-cylinder pressure at each crank angle throughout the entire engine cycle was measured by a pressure transducer installed in the spark plug and a crank angle encoder. The data acquisition system was in place to acquire the electrical signal from the pressure transducer continuously and convert it into digital form. The measured pressure data were stored in the computer and accessed using "Indicom" provided by AVL Company. The complete engine experimental setup is shown in figure 2.

Table 3. Engine Specifications

Engine type	: Spark Ignition with MPFI system
Engine Bore Diameter	: 73.5 mm
Engine Stoke length	: 73.5 mm
Capacity	: 624 cc
Compression ratio	: 9.5:1
Spark Timing (MBT)	: 23° CA bTDC

Table 4. Uncertainties of Measuring Quantities

Measuring Devices	Measurand	Accuracy	% Uncertainty
AVL Digas Analyzer	Carbon monoxide (CO) Hydrocarbon (HC) Nitrogen Oxide (NO)	± 0.02% ± 05 ppm ± 10 ppm	± 0.2 ± 0.1 ± 0.2
Load cell unit	Load	± 0.1 kg	± 0.2
Magnetic Speed Sensor	Engine Speed	± 10 rpm	± 0.1
Electronic Weighing Machine	Fuel consumption	± 0.002 kg	± 0.2
Stop Watch	Time taken	± 0.1 sec	± 0.1

V. ENGINE OPERATING PROCEDURE

Initially, the engine was warmed up and stabilized by operating at no-load conditions for 20 minutes at a speed of 2500 rpm. The experiment was conducted in an environment having a temperature of 32°C and humidity of 70%. The study was performed at five different load conditions, such as 8, 6.4, 4.8, 3.2, and 1.6 kW. The measurements taken at each load condition are the amount of fuel consumed for 60 sec; exhaust gas products like CO, HC, and NO; in-cylinder pressure values for 100 consecutive engine cycles. All the readings were taken three times at each condition, and the averaged value was considered for the performance and emission analysis. The di-gas analyzer probe was purged down completely every time before going for the next measurement to remove all the exhaust gases present in it. The 100 cycles of recorded pressure data were averaged. Subsequently, heat release rates were calculated from the averaged pressure values by applying the equation of the first law of thermodynamics with the help of the in-built software present in the AVL Indicom software. The uncertainties present in measuring quantities are calculated and given (table 4).

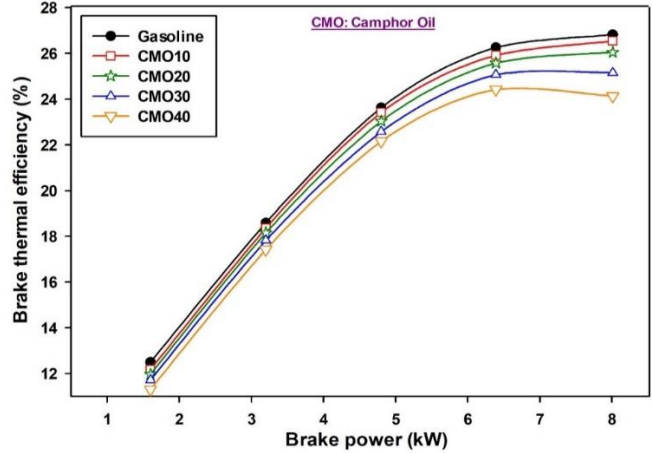## VI. RESULT AND DISCUSSION
A. Brake Thermal Efficiency (BTE)

Fig. 3 Trends of BTE (%) for CMO blends and gasoline at various brake powers

The BTE trend of gasoline and CMO blends at tested engine brake power is shown in figure 3. It is observed that the BTE increases with engine brake power. At higher brake powers, the temperature and pressure are high inside the engine cylinder, which leads to a better combustion process. Also, the air-fuel ratio is maintained closer to stoichiometric ($\Phi \sim 1$) or slightly rich ($\Phi \sim 1.1$) ratio at mid load ranges (6.4 kW, 4.8 kW, 3.2 kW) whereas at low (1.6 kW) and higher loads (8 kW), the engine runs at rich air-fuel ratio ($\Phi \sim 1.2$). This results in incomplete combustion. This is why there is no steep increase observed in the BTE trend (see fig. 3) beyond 6.4 kW [23]. The CMO blends resulted in inferior engine performance when compared to neat gasoline. The BTE trend of the CMO10 blend is comparable to that of gasoline. The BTE of CMO10 at 1.6 kW and 8 kW engine brake power is 12.17% and 26.54%, whereas gasoline is 12.49% and 26.82%, respectively.

Further increase in the CMO proportions in the blend decreases the BTE. The CMO40 blend gives the lowest brake thermal efficiency. This is because the inimical effect created by high viscosity, density, and boiling point of CMO on the fuel flow, spray formation, and evaporation process is more predominant beyond 10% CMO blend, which adversely affects the air-fuel mixture formation and results in an inefficient combustion process [20]. The impact of these adverse effects on the combustion process gets increases with higher CMO blend concentration. The difference in BTE between gasoline and CMO blends at low and mid load is lesser than that at higher loads. This is due to the injection of a large quantity of fuel at higher loads, which have experienced a greater impact of the aforementioned adverse effects on the mixture formation and the combustion process. At 8 kW, the BTE of CMO10, CMO20, CMO30, and CMO40 is 26.54%, 26.05%, 25.15%, and 24.13%, respectively, which are lesser than gasoline, whose value is 26.82%.

B. Brake Specific Fuel Consumption (BSFC)

The BSFC of gasoline and CMO blends are compared in figure 4. The BSFC curve shown a decreasing trend with increasing brake power. The BSFC of CMO10 is nearly close to that of neat gasoline because of insignificant changes observed in gasoline's fuel properties after the blending of CMO by about 10%. Since the calorific value of CMO is 16.5% lesser than gasoline, the blending of CMO beyond 10% with gasoline significantly reduced the calorific value of CMO blends. The decrease in the calorific value with an increase in CMO concentration in the blend is accountable for increases in BSFC of CMO20, CMO30, and CMO40 test fuels. Also, the higher viscosity and density nature of CMO affects the atomization process. The results are large sized fuel droplets that take a longer time for the complete evaporation of fuel, and the higher boiling point of CMO further delays the evaporation rate. The delay in fuel evaporation reduce the air-fuel mixture formation and results in improper combustion. Since the test is performed in a PFI engine, the above factors might increase the wall film thickness formed on the intake port area present behind the intake valve during the fuel injection process. Thus, increasing the BSFC for CMO blends.
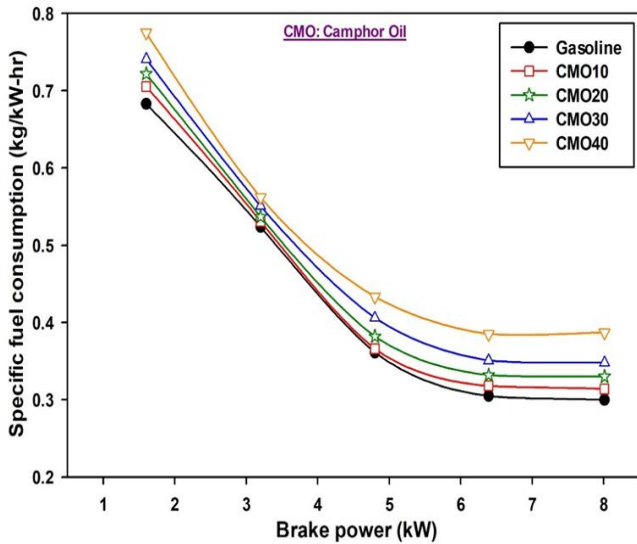

Fig. 4 Trends of BSFC for CMO blends and gasoline at various brake powers

C. Carbon Monoxide Emission (CO)

Figure 5 shows the CO emission given by gasoline and CMO blends at various brake powers. The flame front zone and quench layer outer edge are regarded as CO formation region. Equivalence ratio and temperature are the key parameters that influence the formation and oxidation of CO. CO emissions are mainly associated with the fuel-rich mixture, and dissociation occurs during a lean mixture's burning. The CO emission curve decreases steeply from low load to mid load range and then increase gradually at higher load conditions for all the test blends. At initial load (1.6 kW), the CO emission is very high because it runs with a fuel-rich mixture to have stable combustion. Then, at a higher load (8 kW), CO is again increased gradually because of the increase in fuel injection quantity and reduced resident time to completely oxidize all the CO formed to CO_2 [22,24]. At mid load (4.8 kW), the lowest CO emission of 0.74%, 0.75%, 0.77%, 0.78% and 0.8% for gasoline, CMO10, CMO20, CMO30 and CMO40 is observed respectively. The CO emission of a 10% CMO blend is almost equivalent to that of sole gasoline. Further increasing the CMO ratio in the blend, the CO emission increases irrespective of load condition. Among the CMO blends, CMO40 gives the highest CO emission. The CO emission of CMO40, CMO30, CMO20, CMO10 and gasoline at 8 kW are 0.88%, 0.85%, 0.83%, 0.81% and 0.8% respectively. The CO emission of CMO40 at 1.6 kW load is 1.11% by volume, which is higher by about 5% given by the neat gasoline. The increase in CO with CMO blends is due to the formation of locally fuel-rich regions resulting from poor mixture formation caused by the CMO fuel properties discussed in section 6.1. Even though oxygen is present in the molecular structure of CMO, their efforts to reduce the CO emission by supplying excess oxygen for CO oxidation do not seem to be significant.
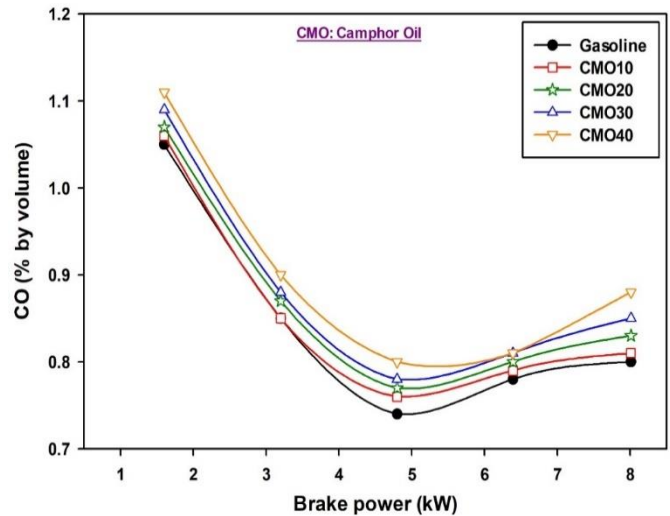

Fig. 5 Trends of CO emission for CMO blends and gasoline at various brake powers

D. Hydrocarbon Emission (HC)

The HC emission trend for the test blends at various engine loads is displayed in figure 6. The flame quenching at the cylinder walls, flow of unburned mixture into crevices volume, incomplete combustion, and absorption and desorption of fuel from the oil deposits are the major causes of HC emission. The HC emission given by gasoline decreases with an increase in brake power and reaches a minimum at 6.4 kW engine load and increases at maximum load condition. All the biofuel blends follow the same trend. The engine runs with a fuel-rich mixture at staring load and maximum load conditions and moves closer to stoichiometric ratio at mid load ranges. The HC emission of CMO10 is nearly close to gasoline at low engine loads, whereas, at higher loads, it is slightly higher than gasoline. At 8 kW, gasoline and CMO10 result in HC emission of 63 and 65

ppm, respectively. The test blends with a higher percentage of camphor oil give a higher amount of HC emission. At full load, the HC emission of CMO20, CMO30, and CMO40 are 66, 68, and 70 ppm, respectively. The increase in HC emissions with CMO blends is partial burning resulting from improper mixture formation and slow burn rate. Since the burn rate depends on the air-fuel ratio, the formation of locally Fuel rich regions due to improper mixing slows down the fuel burning rate and results in bulk gas quenching. This led to incomplete combustion and increased the HC emission for CMO blends. The impact of bulk gas quenching is greater at low engine loads than higher loads that result in a higher amount of HC emission, which is seen in fig. 6.
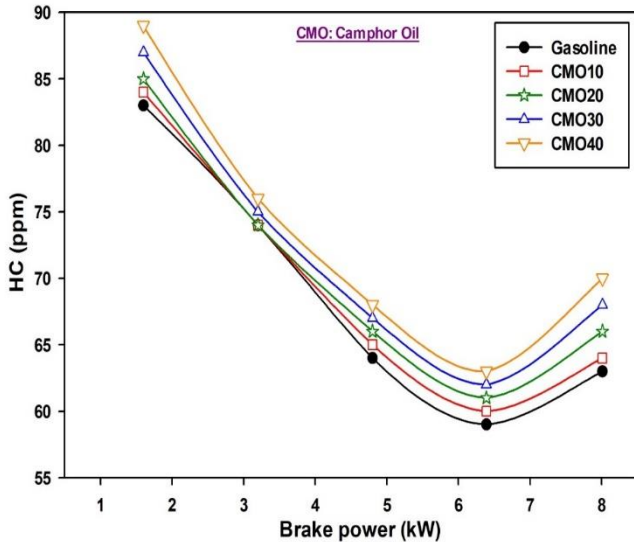

Fig. 6 Trends of HC emission for CMO blends and gasoline at various brake powers

E. Nitrogen Oxides Emission (NOx)

Figure 7 depicts the NOx emission trends for CMO blends and gasoline at various brake powers. NOx emission formation hugely depends on the temperature and oxygen concentration available at the time of combustion. From the NOx graph, it is observed that NOx increases with engine brake power. This is because the pressure and temperature inside the engine cylinder are higher at higher load conditions. At full load, NOx emissions of CMO10, CMO20, CMO30, and CMO40 are lesser by about 2.6%, 6.1%, 11.7%, and 17.6% compared to the sole gasoline value is 340 ppm. The downfall in NOx emission with an increase in CMO percentage in the blend is because of incomplete combustion associated with CMO blends, which reduced the peak pressure (see fig. 8) and subsequently the maximum combustion temperature. Also, higher vaporization enthalpy of CMO than gasoline might induce a cooling effect, which reduces the combustion temperature. These two reasons masked the NOx formation and reduced the NOx emission in the exhaust.
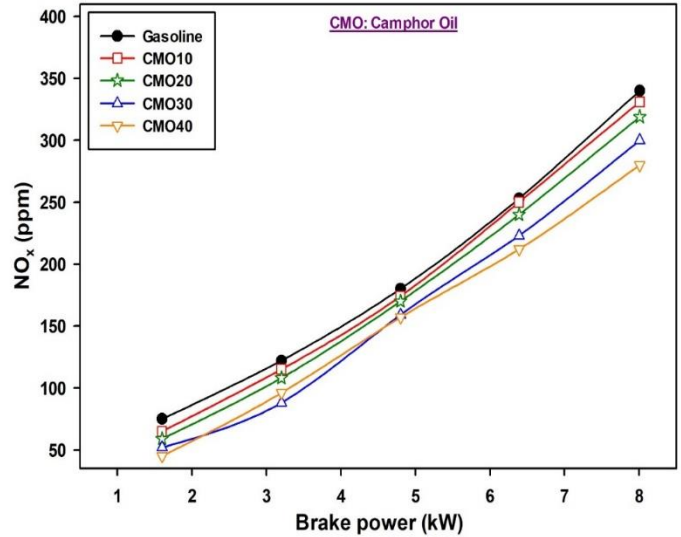

Fig. 7 Trends of NOx for CMO blends and gasoline at various brake powers
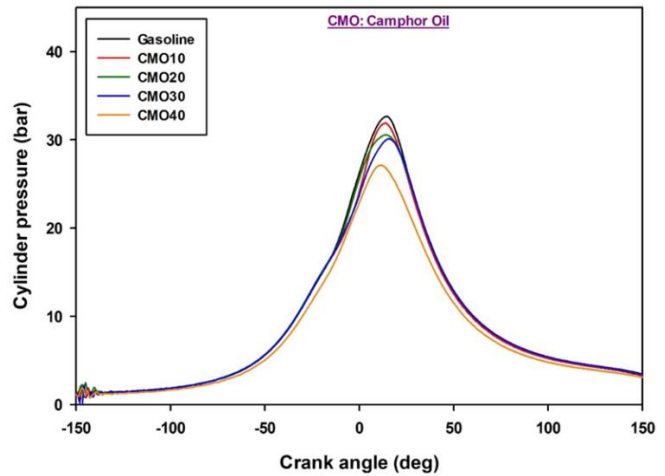
F. Engine Cylinder Pressure

Fig. 8 Engine cylinder pressure at various crank angles for CMO blends and gasoline at 8 kW

The engine cylinder pressure as a function of crank angle for gasoline and CMO blends at 8 kW engine brake power is shown in figure 8. It is observed that the start of ignition is delayed with an increase in CMO content in the blend due to higher flash point, autoignition temperature, and single boiling point nature shown by CMO when compared to sole gasoline. Higher viscosity and density of CMO might have increased the physical delay for CMO blends compared to neat gasoline. The peak in-cylinder pressure decreases when the CMO proportion in the blend increases. The peak pressure is gasoline, CMO10, CMO20, CMO30, and CMO40, 32.643, 31.89, 30.56, 30.10, and 27.10 bar, respectively. The inferior fuel properties of CMO reduced the mixing rate and results in improper air-fuel distribution inside the engine cylinder. This, in turn, reduced the burning rate and subsequently results in partial combustion. The

lesser calorific value of CMO when compared to gasoline also contributes to the overall reduction in combustion pressure and temperature. The crank angle position corresponds to peak pressure is delayed for all CMO blends except CMO40. The reason for the delay is the slow-burning rate associated with CMO blends. Generally, combustion duration increases with a slow-burning rate. But in this case, it is observed in figure 8 that CMO blends show reduced combustion duration. This might be because of flame extinction resulting from the drop in temperature and pressure, which occurs due to the slow-burning rate of CMO blends.

G. Heat Release Rate (HRR)

The heat release rate comparison between gasoline and CMO blends at full load is shown in figure 9. It is inferred that the heat release rates are higher for gasoline compared to the CMO blends. Among the CMO test blends, the CMO10 gives comparable HRR values to that of gasoline. The peak HRR decreases with an increase in the CMO blend percentage. The peak HRR of gasoline, CMO10, CMO20, CMO30, and CMO40 are 81.37, 79.90, 78.45, 78.38, and 78.03 kJ/m3 deg. The delay in the start of combustion observed with CMO blends might have reduced the peak of the HRR. Also, the slowing burning rate and incomplete combustion due to improper mixture formation reduced the overall heat release rates for the CMO blends.
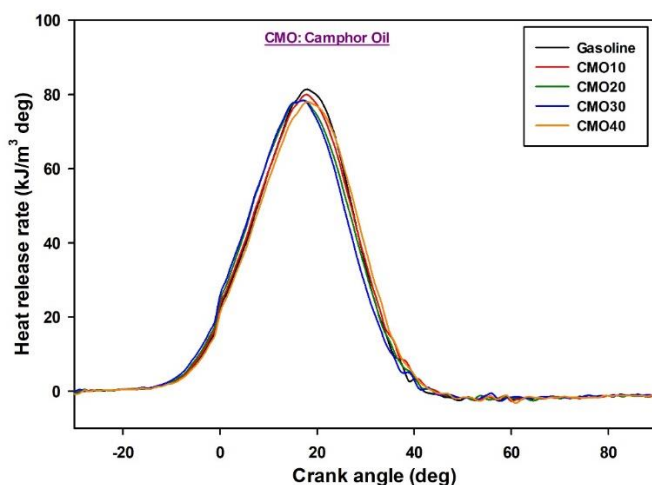

Fig. 9 Heat release rate at various crank angles for CMO blends and gasoline at 8 kW

VI. CONCLUSIONS

The camphor oil's fuel properties are measured to find out its suitability as an alternate fuel to gasoline. Then GC_MS analysis is performed on the extracted camphor oil, and the results show the presence of aliphatic and aromatic hydrocarbon in it. The blend stability test proves that the camphor oil has shown good miscibility and forms a stable blend with gasoline. Finally, the effect of blending camphor oil with gasoline on the performance, emission, and combustion characteristics of a spark-ignition engine is investigated experimentally. Among the CMO blends, the CMO10 almost matches the performance of the gasoline. The experimental results are enumerated as follows:

1. At maximum load, the BTE given by CMO10 is 26.54%, close to gasoline, whose value is 26.82%. The CMO40 gives the lowest BTE, which is equal to 24.13%.

2. The NOx emission decreases, whereas CO and HC increase with the blend's increase in CMO concentration.

3. The peak pressure of gasoline and CMO10 is 32.64 and 31.89 bar, respectively, with crank angle position, the peak pressure is the same for both.

4. Among the CMO blends, CMO10 gives the maximum heat release rate of 79.90 kJ/m3 deg, which is slightly lesser than the gasoline, whose value is 81.73 kJ/m3 deg. The CMO40 gives the lowest peak heat release rate of 78.03 kJ/m3 deg.

The camphor oil has shown the capacity to replace gasoline by about a maximum of 10% by volume. Even though a 10% CMO blend results in slightly lesser performance than gasoline, a slight engine modification such as a high-pressure injector, early injection timing, piston modification, or adding an additive to camphor oil blends might improve the engine performance. These improvements can be taken as the scope of the study and studied in the future.

REFERENCES

[1] Manoj Babu, C.G. Saravanan, M. Vikneswaran, V. Edwin Geo, J. Sasikala, J.S. Femilda Josephin, D. Das, Analysis of performance, emission, combustion and endoscopic visualization of micro-arc oxidation piston coated SI engine fuelled with low carbon biofuel blends, fuel. 285 (2021) 119189. https://doi.org/10.1016/j.fuel.2020.119189.

[2] P. Prabhakaran, C.G. Saravanan, R. Vallinayagam, M. Vikneswaran, N. Muthukumaran, K. Ashok, Investigation of swirl induced piston on the engine characteristics of a biodiesel fueled diesel engine, fuel. 279 (2020) 118503. https://doi.org/10.1016/j.fuel.2020.118503.

[3] Urdhwareshe R. The Automotive Research Association of India, 2 Wheeler Vehicles : BS VI, (2018) 62.

[4] M. Loganathana, A.Anbarasu. , V.M. Madhavan, K. Arun Balasubramanian, V. Thanigaivelan, M. Vikneswaran, Investigation on the effect of diethyl ether with hydrogen-enriched cashew nutshell (CNS) biodiesel in direct injection (DI) diesel engine, fuel. 277 (2020) 118165. https://doi.org/10.1016/j.fuel.2020.118165.

[5] C. Nandakumar, V. Raman, C.G. Saravanan, M. Vikneswaran, S. Prasanna Raj Yadav, M. Thirunavukkarasu, Effect of nozzle hole geometry on the operation of kapok biodiesel in a diesel engine, fuel. 276 (2020) 118114. https://doi.org/10.1016/j.fuel.2020.118114.

[6] Reşitoğlu2015_Article_ThePollutantEmissionsFromDiese.pdf, (2015).

[7] F.P. Sanchez, A. Bandivadekar, J. German, Estimated cost of emission reduction technologies for LDVs, Int. Counc. Clean Transp. (2012) 1–136.

[8] PTI agency, Drop-in petrol, diesel price gap fuel customers' shift towards petrol, CNG cars: ICRA, Econ. Times. (2020). https://energy.economictimes.indiatimes.com/news/oil-and-gas/drop-in-petrol-diesel-price-gap-to-fuel-customers-shift-towards-petrol-cng-cars-icra/76854112.

[9] V. Ravikumar, D. Senthilkumar, C.G. Saravanan, V. Edwin Geo, M. Vikneswaran, C. Solaimuthu, J.S. Femilda Josephin, Study on the

effect of 2-butoxyethanol as an additive on the combustion flame, performance and emission characteristics of a spark-ignition engine, Fuel. 285 (2021) 119187. https://doi.org/10.1016/j.fuel.2020.119187.

[10] A.D. Sagar, Automobiles and global warming: Alternative fuels and other carbon dioxide emissions reduction options, Environ. Impact Assess. Rev. 15 (1995) 241–274. https://doi.org/10.1016/0195-9255(95)91707-F.

[11] G. Archer, T. Earl, E. Bannon, J. Poliscanova, N. Muzi, S. Alexandridou, CO2 Emissions From Cars: The facts, Transp. Environ. (2018) 53. https://www.dbresearch.de/PROD/DBR_INTERNET_EN-PROD/PROD0000000000346332/CO2+emissions+from+cars:+Regul ation+via+EU+Emissio.pdf.

[12] S. Thiruvenkatachari, C.G. Saravanan, V. Edwin Geo, M. Vikneswaran, R. Udayakumar, F. Aloui, Experimental investigations on the production and testing of Azolla methyl esters from Azolla microphylla in a compression ignition engine, fuel. (2020) 119448. https://doi.org/10.1016/j.fuel.2020.119448.

[13] C. Bae, J. Kim, Alternative fuels for internal combustion engines, Proc. Combust. Inst. 36 (2017) 3389–3413. https://doi.org/10.1016/j.proci.2016.09.009.

[14] O.I. Awad, R. Mamat, O.M. Ali, N.A.C. Sidik, T. Yusaf, K. Kadirgama, M. Kettner, Alcohol and ether as alternative fuels in spark ignition engine: A review, Renew. Sustain. Energy Rev. 82 (2018) 2586–2605. https://doi.org/10.1016/j.rser.2017.09.074.

[15] P. Sakthivel, K.A. Subramanian, R. Mathai, Comparative studies on combustion, performance and emission characteristics of a two-wheeler with gasoline and 30% ethanol-gasoline blend using chassis dynamometer, Appl. Therm. Eng. 146 (2019) 726–737. https://doi.org/10.1016/j.applthermaleng.2018.10.035.

[16] P.P. Morajkar, G.D.J. Guerrero Penã, A. Raj, M. Elkadi, R.K. Rahman, A. V. Salkar, A. Pillay, T. Anjana, M.S. Cha, Effects of Camphor Oil Addition to Diesel on the Nanostructures and Oxidative Reactivity of Combustion-Generated Soot, Energy and Fuels. 33 (2019) 12852–12864. https://doi.org/10.1021/acs.energyfuels.9b03390.

[17] A. Manoj Babu, C.G. Saravanan, M. Vikneswaran, V. Edwin Jeo, J. Sasikala, Visualization of in-cylinder combustion using an endoscope in a spark-ignition engine fueled with pine oil blended gasoline, fuel. 263, (2020). https://doi.org/10.1016/j.fuel.2019.116707.

[18] R. Vallinayagam, S. Vedharaj, N. Naser, W.L. Roberts, R.W. Dibble, S.M. Sarathy, Terpineol as a novel octane booster for extending the knock limit of gasoline, fuel. 187 (2017) 9–15. https://doi.org/10.1016/j.fuel.2016.09.034.

[19] A. Biswal, R. Kale, G.R. Teja, S. Banerjee, P. Kolhe, S. Balusamy, An experimental and kinetic modeling study of gasoline/lemon peel oil blends for PFI engine, fuel. 267 (2020) 117189. https://doi.org/https://doi.org/10.1016/j.fuel.2020.117189.

[20] A. Velavan, C.G. Saravanan, M. Vikneswaran, E. James Gunasekaran, J. Sasikala, Visualization of in-cylinder combustion flame and evaluation of engine characteristics of MPFI engine fueled by lemon peel oil blended gasoline, Fuel. 263 (2020) 116728. https://doi.org/10.1016/j.fuel.2019.116728.

[21] G. Kasiraman, B. Nagalingam, M. Balakrishnan, Performance, emission and combustion improvements in a direct injection diesel engine using cashew nut shell oil as fuel with camphor oil blending, Energy. 47 (2012) 116–124. https://doi.org/10.1016/j.energy.2012.09.022.

[22] V.E. Geo, D.J. Godwin, S. Thiyagarajan, C.G. Saravanan, F. Aloui, Effect of higher and lower order alcohol blending with gasoline on performance, emission and combustion characteristics of SI engine, fuel. 256 (2019) 115806. https://doi.org/10.1016/j.fuel.2019.115806.

[23] M. Vikneswaran, C.G. Saravanan, J. Sasikala, Endoscopic visualization of combustion flame to study the effect of 1,4-dioxane as an additive on the spatial flame characteristics of spark ignition engine, fuel. 276 (2020) 118072. https://doi.org/10.1016/j.fuel.2020.118072.

[24] D. Jesu Godwin, V. Edwin Geo, S. Thiyagarajan, M. Leenus Jesu Martin, T. Maiyalagan, C.G. Saravanan, F. Aloui, Effect of hydroxyl (OH) group position in alcohol on performance, emission and combustion characteristics of SI engine, Energy Convers. Manag. 189 (2019) 195–201. https://doi.org/10.1016/j.enconman.2019.03.063.

[25] Hassan Babiker, Babiker.A.Karma, Adil. A.Mohammed , AspenHysys Simulation of Methanol to Dimethylether (DME), International Journal of Engineering Trends and Technology (IJETT), V46(4),(2017) 214-220.